Inner-Shell Spectroscopy and Imaging of a Subbituminous Coal: In-Situ Analysis of Organic and Inorganic Microstructure Using C(1s)-, Ca(2p)-, and Cl(2s)-NEXAFS

ARTICLE *in* ENERGY & FUELS · MAY 1995

Impact Factor: 2.79 · DOI: 10.1021/ef00051a018

6 AUTHORS, INCLUDING:

Harald Werner Ade
North Carolina State University
359 PUBLICATIONS **8,688** CITATIONS

SEE PROFILE

Inner-Shell Spectroscopy and Imaging of a Subbituminous Coal: In-Situ Analysis of Organic and Inorganic Microstructure Using C(1s)-, Ca(2p)-, and Cl(2s)-NEXAFS†

George D. Cody* and Robert E. Botto

Chemistry Division, Argonne National Laboratory, Argonne, Illinois 60439

Harald Ade

Department of Physics, North Carolina State University, Raleigh, North Carolina 27695

Sutinder Behal and Mark Disko

Corporate Research Science Laboratory, Exxon Research and Engineering Laboratory, Annandale, New Jersey 08801

Susan Wirick

Department of Physics, SUNY at Stony Brook, Stony Brook, New York 11794

Received October 18, 1994. Revised Manuscript Received February 13, 1995⊗

Inner-shell microspectroscopy has been used to provide in-situ microanalysis of organic and inorganic constituents within Wyodak subbituminous coal (APCS No. 2). Two specimens were prepared, one loaded with Ca^{2+} and the other rinsed in HCl. Carbon NEXAFS spectroscopy was used to determine the chemical structure of liptinitic and huminitic macerals. Liptinite was characterized by an abundance of aliphatic carbon, evident by the intensity of absorption assigned to the transition from carbon's 1s orbital to a mixed valence/Rydberg state; a low concentration of aromatic carbon, evident by low-intensity absorption associated with a $1s-\pi^*$ transition; and an appreciable quantity of carboxylic functionality, evident through a relatively intense absorption associated with a $1s-\pi^*$ transition due to C=O. The huminite exhibits fine structure indicative of an abundance of both aromatic and aliphatic carbon. The presence of polyhydroxylated aromatic carbon and carbonyl associated with carboxylic acids is also clearly indicated. In addition to carbonaceous heterogeneities, chlorine-rich inclusions were also identified. These were observed to strongly absorb in the energy range near 270 eV corresponding to Cl's 2s absorption edge. The inclusions are anticipated to be inorganic chlorides, precipitates which formed following the rinse in dilute HCl. Imaging and spectroscopy on the calcium's 2p absorption edge reveals that the chloride's cation is not calcium, although calcium is detected in the huminite of the Ca^{2+}-loaded coal.

Introduction

Analysis of the chemistry of coals is hindered by the fact that coal is a composite of organic and inorganic constituents assembled at a very fine scale. Recently we have demonstrated that X-ray inner-shell spectroscopy was capable of revealing chemical structural information in coal at a scale sufficiently fine to characterize these different constituents.[1,2] In these initial investigations, X-ray microspectroscopy was applied to the analysis of a high-volatile A rank coal using a scanning transmission X-ray microscope (STXM) located at the National Synchrotron Light Source at Brookhaven National Laboratory. In the second paper,[2] the focus was primarily on assigning the fine structure at carbon's K edge, which results from photoinduced transitions of carbon's 1s electrons to various bound states (low-lying unoccupied molecular orbitals, LUMO's), to the presence of various functional groups.

Analysis of the carbon 1s spectrum of different maceral classes revealed distinctly different near-edge X-ray absorption fine structure (NEXAFS) consistent with fundamental differences in their chemical structures.[2] In particular, the relative intensity of two pronounced features were observed to be characteristic of the maceral type. At the lowest energies, near 285.5 eV, an absorption band appears which is assigned to the photoinduced transition of an electron from carbon's 1s orbital to the lowest lying aromatic π^* molecular orbital. The second feature was a pronounced shoulder on the absorption edge at a slightly higher energy, $E \sim 288$ eV.

† This work was performed under the auspices of the Office of Basic Energy Sciences, Division of Chemical Sciences, U.S. Department of Energy under contract no. W-31-109-38.

⊗ Abstract published in *Advance ACS Abstracts,* April 15, 1995.

(1) Botto, R. E.; Cody, G. D.; Ade, H.; Behal, S.; Disko, M.; Wirick, S. *Energy Fuels* **1994**, *8*, 51.

(2) Cody, G. D.; Botto, R. E.; Ade, H.; Behal, S.; Disko, M.;Wirick, S. *Energy Fuels* **1995**, *9*, 75.

0887-0624/95/2509-0525$09.00/0

This feature was assigned to a 1s transition to a mixed Rydberg/C−H* (antibonding, σ_{C-H}*) state.[3] The intensity of this absorption band was shown to correlate, positively, with the concentration of sp^3-hybridized carbon.

In the case of cutinite (a liptinitic maceral derived from selective preservation of waxy leaf coating, cutin) the intensity of absorption due to the 1s-Rydberg/C−H* was considerably more intense than that due to the 1s−π* absorption, while the opposite was true for vitrinite.[2] Across the assemblage of macerals contained within high-volatile A bituminous coal, the ratio of the 1s−π* to the 1s-Rydberg/C−H* absorption intensities was observed to be low (≪1.0) for cutinite, above 0.5 in the case of sporinite, ~1.2 for vitrinite, and greatest for fusinite, ~1.4.[2]

Aside from our analysis of sedimentary organic matter, others have applied STXM to the analysis of the carbon edge of a variety of microheterogeneous materials. These studies include the analysis of wet chromosomes,[4] freeze-dried fibroblast cells,[5] and polymer blends.[6] In the present report inner-shell microspectroscopy is applied to probe the chemistry of a low-rank coal, APCS No. 2, obtained from the Wyodak-Anderson subbituminous coal reserves. Results of the earlier C-NEXAFS analyses suggest that the chemistry of low-rank coals would prove to be especially interesting due to the broader range of functional groups, more oxygen functionality in particular, and the bulk matter within these coals, the maceral huminite, is derived from principally angiosperm lignin.[7] This latter point, although subtle, implies that the average degree of hydroxylation of aromatic moieties should be greater than similar rank huminite derived from exclusively gymnosperm lignin.

In addition to the increased complexity of the carbon chemistry, the relatively high concentration of acidic functional groups in the low-rank coal suggests that the detection of chelated inorganics in coal might be used as a basis for contrast for imaging purposes.

Within the energy range available to the X-ray microscope both the calcium's 2p and chlorine's 2s absorption edges are accessible. While imaging with the monochromator tuned to calcium's 2p absorption edge has been used to document calcium loss in bone,[8] imaging near chlorine's 2s absorption edge has, to the best of our knowledge, not been explored previously using the STXM. In the present experiments, imaging of calcium-loaded coals is explored as a means to determine whether discrete domains rich in exchangeable inorganics could be identified. Imaging on the chlorine edge is used to detect the presence of chlorides.

Experimental Section

Sample. The present investigation focused exclusively on a sample of subbituminous B rank coal, APCS No. 2, obtained through the Argonne Premium Coal Sample Bank. The analytical data for this coal is presented in Table 1. It is important to note, however, that individual blocks of coal were selected for the purpose of preparing thin sections for X-ray microanalysis. It is acknowledged, therefore, that the individual samples analyzed in the present study may not be representative of the Wyodak seam or even APCS No. 2, as a whole.

Table 1. Characteristics of Wyodak Subbituminous Coal: APCS No. 2

% C[a]	% H	% O	% S	% ash	% vit[b]	% lip[c]	% inrt[d]
75	5.4	18	0.6	9.0	89	<1	11

[a] C, H, O, and S on a dry ash free, weight percent basis. [b] Vitrinite, in lower rank coals typically referred to as huminite. [c] Liptinite. [d] Inertinite.

Sample Preparation. Very thin sections of coal were prepared using an ultramicrotome. Sample thickness were estimated to be on the order of 100−200 nm. This range is excellent for both spectroscopy and imaging purposes. The inevitable microtoming artifacts were principally in form of microcracks and a small amount of scoring. Such artifacts were, however, unambiguously assigned and their presence did not interfere with the identification of compositionally discrete microdomains. Details on various aspects of the sample preparation have been described previously.[2]

Ion Exchange. The capacity of lower rank coals to bind cations has been well established.[9,10] One of the goals of the present experiments was to image any heterogeneities in spatial distribution of chelating groups in this coal. Two samples of APCS No. 2 were selected for analysis, these were fabricated into thin (~1 mm cross section) pillars, and immersed in dilute HCl for 1 week to displace the majority of exchangeable cations. Following acidification, both samples were immersed in distilled water for 1 week. One of the samples was then immersed in a dilute solution of calcium hydroxide for nearly a week and finally rinsed in distilled water. The physical integrity of the sample was not compromised by this procedure.

Carbon, Calcium, and Chlorine NEXAFS. The scanning X-ray microscope (STXM) is located at the X1A beam line at the National Synchrotron Light Source at Brookhaven National Laboratory. In its current configuration, the STXM is capable of an energy resolution of 0.3 eV and spatial resolution of 55 nm. X-ray microfocusing is accomplished with diffraction limited optics using a Fresnel zone plate and an order sorting aperture.[11]

The accessible energy window at X1A is limited by the design of the monochromator, which generates X-rays in the wavelength range of ~1.5−5 nm.[12] Included within this energy range are carbon's 1s (280−320 eV), chlorine's 2s (260−280 eV), and calcium's 2p (340−380 eV) absorption edges. Spectra and images were obtained with the undulator gap optimized to span the characteristic energy ranges of each of these elements. Additional details regarding STXM are available in the literature.[11,12]

Results and Discussion

Carbon Spectroscopy and Imaging. The sample of APCS No. 2 selected for the present experiment is composed predominantly of huminite, a precursor to vitrinite.[13] Although inertinite has been reported to be

(3) Hitchcock, A. P.; Newbury, D. C.; Ishii, I.; Stöhr, J.; Horsley, J. A.; Redwing, R. D.; Johnson, A. L.; Sette, F. *J. Chem. Phys.* **1986**, *85*, 4849.
(4) Williams, S.; Zhang, X.; Jacobsen, C.; Kirz, J.; Lindass, S.; Van't Hof, J.; Lam, S. S. *J. Microsc.* **1993**, *170*, 155.
(5) Zhang, X.; Williams, S.; Jacobsen, C.; Kirz, J.; Fu, J.; Wirick, S., manuscript in preparation.
(6) Ade, H. *Synchr. Rad. News* **1994**, *7*, 11.
(7) Hatcher, P. G., personal communication.
(8) Buckley, C. J.; Foster, G. F.; Burge, R. E.; Ali, S. Y.; Scotchford; C. A., Kirz, J.; Rivers, M. L. *Rev. Sci. Instrum.* **1992**, *63*, 588.
(9) van Krevelan, D. W. *Coal*, 3rd ed., Elsevier: New York, 1992.
(10) Gorbaty, M. L. *Fuel* **1978**, *57*, 797.
(11) Jacobsen, C.; Williams, S.; Anderson, E.; Browne, M. T.; Buckley, C. J.; Kern, D.; Kirz, J.; Rivers, M.; Zhang, X. *Opt. Commun.* **1991**, *86*, 351.
(12) Kirz, J.; Ade, H.; Jacobsen, C.; C.-H. Ko, Lindass, S.; Mcnulty, I.; Sayre, D.; Williams, S.; Zhang, X. *Rev. Sci. Instrum.* **1992**, *63*, 557.
(13) Stach, E.; Mackowsky, M.-Th., Teichmüller, M.; Taylor, G. H.; Chandra, D.; Teichmüller, R., *Stach's Textbook of Coal Petrology*, 3rd ed., Gebruder Borntraeger: Stuttgart, Germany, 1982.

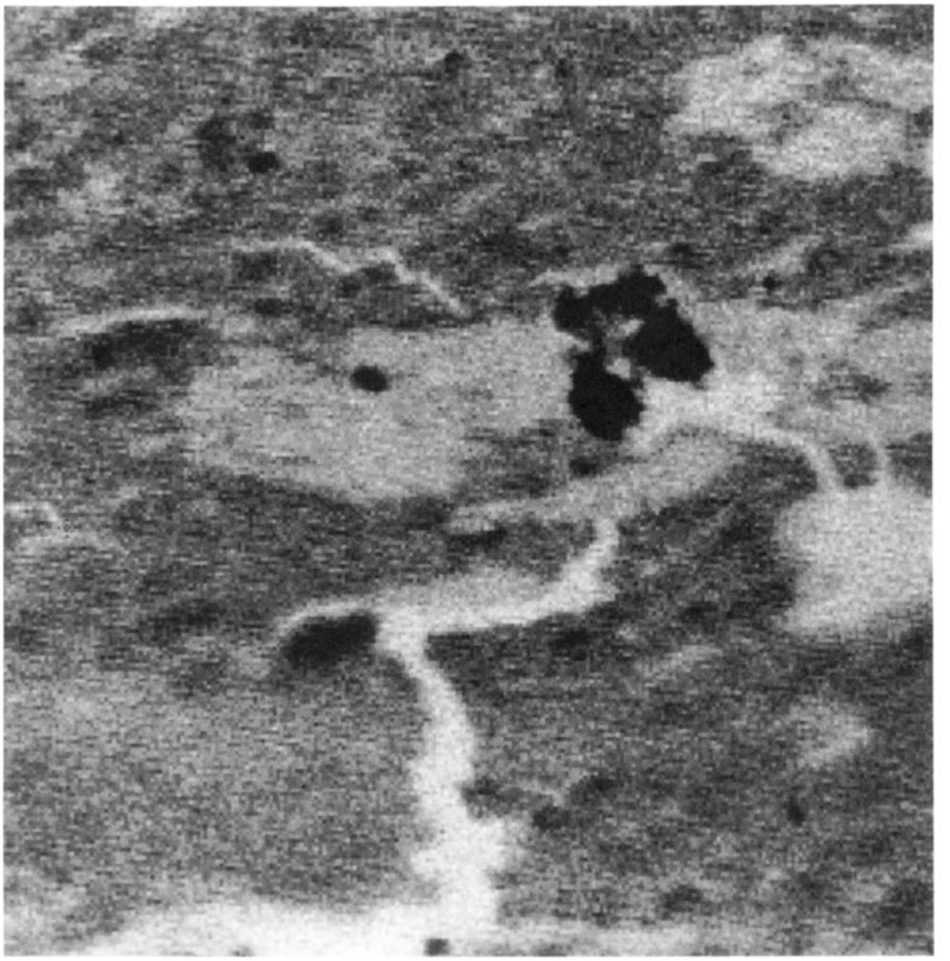

Figure 1. X-ray image of a selected region in APCS No. 2 containing huminite and liptinite. The monochromator is tuned to 285.5 eV. In the center and upper right corner of the image are liptinitic macerals, evident by their low absorbance at this energy. The matrix material is the maceral huminite. A microcrack is clearly evident in the middle of the image. The strongly absorbing region (center right) is an inorganic inclusion.

the second most abundant maceral in this coal, 11% based on petrographic analysis,[14,15] inertinite was not present in any of the sections used in the present study. Figure 1 presents an image of a section of APCS No. 2, obtained with the monochromator tuned to 285.5 eV. Clearly evident in the center of the image is a maceral exhibiting high X-ray transmission, diagnostic of a liptinitic maceral.[2] Another liptinitic maceral is evident in the upper right hand corner of Figure 1.

Liptinitic macerals constitute only a small fraction of the total maceral content in this coal and it was fortunate to have located these. Petrographic analysis of the liptinitic macerals within the Wyodak-Anderson coals have shown that cutinite and sporinite are the dominant liptinitic macerals, while lesser amounts of resinite have also been identified.[15] The morphology of the liptinites in Figure 1 is suggestive of resinite. Certainly their morphology discredits assignment as cutinite; however, with so few specimens to compare one cannot be more definitive in discounting sporinite.

Surrounding these liptinitic regions in Figure 1 is huminite, the matrix maceral of this sample. A salient feature in Figure 1 is the strongly absorbing region adjacent to the center liptinite; similar inclusions or particles were observed throughout the samples. Subsequent analysis indicates that these regions are inorganic and not carbonaceous, as will be discussed in detail below. The remaining features in Figure 1 are microcracks that are clearly evident with characteristically high X-ray transmission and jagged outlines.

The significant differences in carbon chemistry of liptinite and huminite in APCS No. 2 are revealed when an image of the region is reacquired while the monochromator is tuned to 288.1 eV (Figure 2). Both liptinitic macerals (Figure 1) are now observed to have the lowest X-ray transmission. Similar contrast reversals have been observed for liptinitic macerals in the high volatile A rank coal.[1,2]

The basis for the contrast reversal, observed in Figures 1 to 2, is clearly indicated by comparing the inner-shell spectra of the two macerals. The carbon inner-shell spectrum of huminite is presented in Figure 3. Several clearly defined absorption bands are evident across the spectrum. At the lowest energy, $E \sim 285$ eV, a pronounced absorption band appears which is assigned to the $1s-\pi^*$ transition for aromatic carbon. A well-defined shoulder is present near 287 eV as well as other pronounced absorption bands at $E \sim 289$ and 294 eV.

Liptinite's carbon spectrum (Figure 4) is dominated by very strong absorption at $E \sim 288$ eV and several

(14) Vorres, K. S. *Users Handbook for the Argonne Premium Coal Sample Program*; National Technical Information Service, U.S. Dept. of Commerce: Springfield, VA, 1994.
(15) Davis, A., personal communication.

Figure 2. X-ray image of the interesting region with the monochromator now tuned to 288.1 eV. Liptinites now strongly absorb. Note that the inorganic inclusions no longer exhibit the strongest absorption.

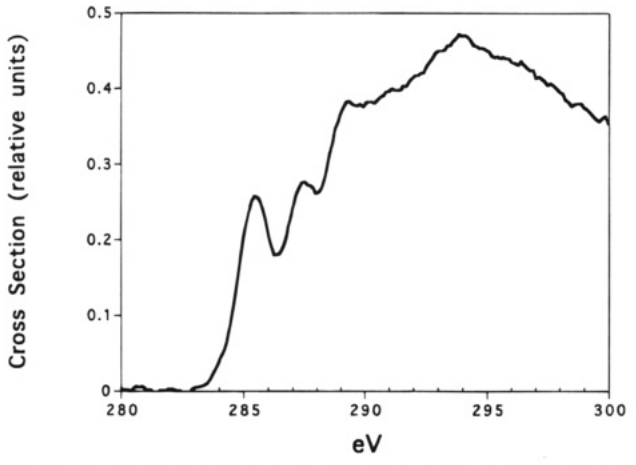

Figure 3. C-NEXAFS spectrum of huminite. Intense bands associated with aromatic, hydroxylated aromatic carbon, and aliphatic carbon are clearly evident.

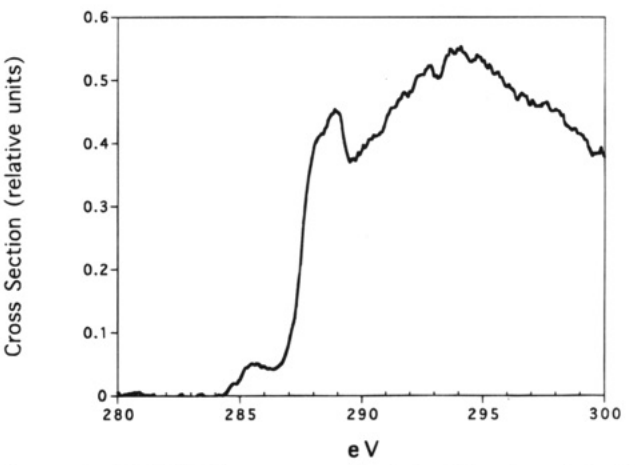

Figure 4. C-NEXAFS spectrum of liptinite. Note the minimal intensity of the $1s-\pi^*$ absorption band near 285.5 eV and the very intense mixed valence/Rydberg absorption band near 288 eV.

broad absorption bands near 294 eV. The most striking differences between the carbon spectra of the two macerals (Figure 4) is the extremely low intensity of the $1s-\pi^*$ absorption associated with sp^2-hybridized carbon in liptinite apparent by the small absorption band is centered near 286 eV.

In order to facilitate the assignment of absorption fine structure in Figures 3 and 4 to specific electronic transitions it is helpful to focus exclusively on absorption due to transitions to bound states. Much of the absorption intensity in either spectrum, however, is derived from photoexcitation of the inner-shell electron into the continuum, i.e., beyond the vacuum level. The characteristic shape of a core to continuum transition is that of a step function, i.e., a rapid rise to a plateau. Removal of the contribution from the continuum step from the inner-shell spectrum eliminates distortions in the intensity and shape of absorption bands associated with transitions to bound states proximal to the absorption edge.

The shape of the continuum step may be computed

several different ways. The simplest approach is to use a step function, however an arc tangent or step-error function[16] may provide a more realistic fit to the data. These latter functions take lifetime and instrumental effects into account. In the most physically rigorous applications, the choice of either function would be subject to the detailed aspects of the experimental parameters. As applied in practice, both functions can reproduce the shape of the continuum step. For the present purposes, therefore, the arc tangent function will be applied.

The magnitude, $I(E)$, and shape of a continuum step is determined by the following equation[16]

$$I(E) = H\left[\frac{1}{2} + \frac{1}{\pi}\arctan\left(2\frac{(E-P)}{\Gamma}\right)\right] \qquad (1)$$

where H is the height of the step, E is energy in eV, P is ionization potential, and Γ is the width at half-height of the transition.

In the case where a number of chemically inequivalent carbons are present, several continuum steps (corresponding to different ionization potentials) are required to faithfully fit the absorption edge data. Aromatic carbon has its ionization potential near 290.3 eV,[17] aliphatic carbon has its ionization potential near 290.5 eV,[3,18] hydroxylated aromatic carbon has its ionization potential near 292 eV,[17] aldehyde's ionization potentials are near 293–294 eV,[19,20] and carboxylic acid's ionization potential are in the range of 295–296 eV.[21,22]

In practice, one cannot accurately simulate the intensity and positions of the continuum steps without detailed knowledge of the carbon chemistry. This is clearly a problem in the case of a complex natural product such as coal. For the present purposes, therefore, the position and intensity of the continuum steps will be selected using simplifying assumptions regarding the localized carbon chemistry. The extent to which these assumptions introduce uncertainty in the assignment of a given bound state transition will be considered.

In the case of huminite, the contribution to the absorption spectrum was simulated with two continuum steps, each with Γ = 1.0 eV. Their magnitude was assessed by the atomic ratio of carbon to oxygen in APCS No. 2 (Table 1). Carbon bonded to oxygen is accounted for with a ionization threshold at 292 eV and 15% of the total continuum intensity. The remaining aliphatic and aromatic carbon is accounted for with an ionization threshold at 290.4 eV and 85% of the continuum intensity. In the case of the liptinite, 100% of the continuum intensity was assigned to carbon with an ionization threshold at 290.5 eV, Γ = 1.0 eV. Subtraction of these contributions from the huminite and liptinite spectra (Figures 3 and 4) yields the absorption structure due to transitions to bound states exclusively and is presented in Figures 5 and 6, respectively. It should be noted that while in both cases the pronounced fine structure below 290 eV is unaffected by our choices for the position of the continuum steps, the intensity and peak shape of high-energy absorption bands is dependent on the assumptions regarding the position and intensity of the continuum steps.

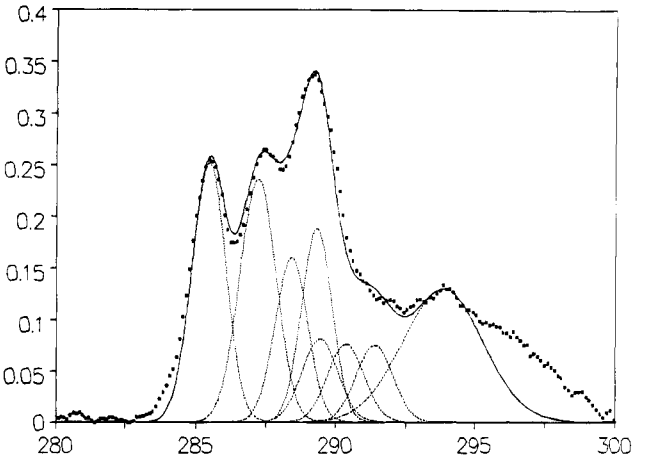

Figure 5. Continuum corrected C-NEXAFS spectrum of huminite, where the contribution to the total intensity from ionization to the continuum has been subtracted. Deconvolution yields eight component absorption bands (Table 2).

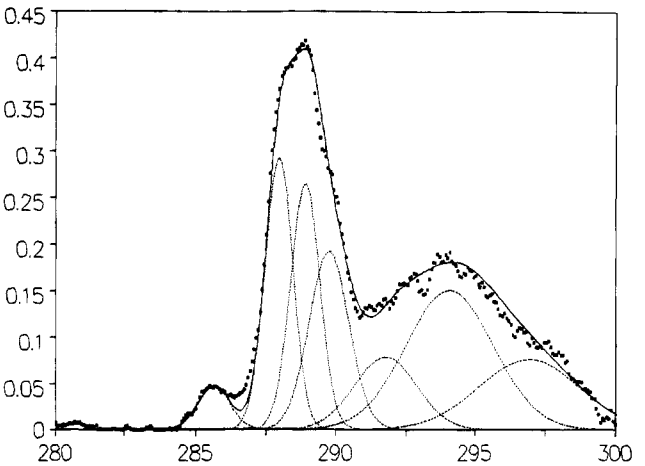

Figure 6. Continuum corrected C-NEXAFS spectrum of liptinite, where the contribution to the total intensity from ionization to the continuum has been subtracted. Deconvolution yields seven component absorption bands (Table 2).

First, consider the continuum step corrected inner-shell spectrum of huminite (Figure 5), where four prominent absorption bands are clearly resolved. The band assignments are as follows. The lowest energy band near 285 eV is confidently assigned to the $1s-\pi^*$ transition of aromatic carbon bonded to either a proton or carbon (Table 2). Using the electronic states of benzene as an analogue, it is noted that while the lowest energy inner-shell transition is anticipated to be intense, a second, higher energy transition to the highest (in this case) unoccupied molecular orbital is also expected. This transition, sometimes referred to as a $1s-2\pi^*$ transition, is observed to occur approximately 4 eV higher in energy than the $1s-\pi^*$ transition and with nearly one-quarter the intensity.[17] While absorption due to this second transition is not observed directly, its presence is

(16) Stöhr, J. *NEXAFS Spectroscopy*, Springer-Verlag: New York, 1991.
(17) Francis, J. T.; Hitchcock, A. P. *J. Phys. Chem.*, **1992**, *96*, 6598.
(18) Hitchcock, A. P.; Ishii, I. *J. Electron Spectrosc. Relat. Phenom.* **1987**, *42*, 11.
(19) Hitchcock, A. P.; Urquart, S. G.; Rightor, E. G. *J. Phys. Chem.* **1992**, *96*, 8736.
(20) Hitchcock, A. P.; Brion, C. E. *J. Electron Spectrosc. Relat. Phenom.* **1980**, *19*, 231.
(21) Robin, M. B.; Ishii, I.; Mclaren, R.; Hitchcock, A. P. *J. Electron Spectrosc. Relat. Phenom.* **1988**, *47*, 53.
(22) Ishii, I.; Hitchcock, A. P. *J. Electron Spectrosc. Relat. Phenom.* **1988**, *46*, 55.

Table 2. C-NEXAFS of Huminite: Inner-Shell Transition Energies and Assignments

energy (eV)	assignment	carbon functionality
285	$1s-\pi^*$	$C_{AR}-H$, $C_{AR}-C$ (LUMO)
287	$1s-\pi^*$	$C_{AR}-OH$ (phenol) (LUMO)
288	$1s-3p/\sigma_{C-H}^*$	CH_2, CH_3
289	$1s-\pi^*$	C=O (acid, aldehyde)
289[a]	$1s-2\pi^*$	$C_{AR}-H$, $C_{AR}-C$
290[a]	1s−4p	CH_2, CH_3
291[a]	$1s-2\pi^*$	$C_{AR}-OH$ (phenol)
294	$1s-\sigma^*$	C−C (aromatic)
297	$1s-\sigma^*$	C−O (phenol)

[a] The presence of these absorption bands is inferred from the presence of absorption bands assigned to electronic transitions to lower energy UMO's associated with the same carbon core obital.

inferred from the appearance of the 285 eV transition. The $1s-2\pi^*$ absorption band clearly contributes to the intensity of the prominent peak near 289 eV and must be included (Table 2) if quantitative deconvolution of the C-NEXAFS spectrum of coal is required.

An equally prominent absorption band in Figure 5 is centered near 287 eV. This band is assigned to the $1s-\pi^*$ transition of aromatic carbon bonded to oxygen (Table 2), as in the case of phenol or aryl ether. The shift in energy of this transition relative to protonated aromatic carbon results from the higher electron affinity of the substituent and is observed in the inner-shell spectrum of phenol[17] as well in the spectrum of a number of halogenated aromatics.[16,21,23] As was previously the case with benzene, a second transition to the next highest UMO, the $1s-2\pi^*$, is expected near 291 eV(Table 2). It is important to note that the intensity of the 287 eV band is comparable to the intensity of the 285 eV band. The ratio of the intensities of the two $1s-\pi^*$ transitions is greater than that reported for phenol[17] and similar to that which has been reported for hydroxyquinone.[17] This would imply that the average degree of hydroxylation in the huminite is close to 2 OH/ring.

The most intense band in the continuum corrected huminite spectrum is centered near 289 eV. An important contributor to this feature is absorption due to a 1s transition to a mixed Rydberg/C−H* state, centered near 288 eV (Table 2). As discussed previously,[2] the intensity of this transition correlates strongly with the concentration of aliphatic carbon and is indicative of the concentration of methyl and methylene groups in huminite.

Other functional groups also contribute to the absorption intensity near 289 eV. Aromatic and aliphatic carboxylic acids are anticipated to be present in low rank huminitic macerals.[9] The $1s-\pi^*$ transitions associated with the C=O of the acid have particularly large oscillator strengths and contribute significant absorption intensity near 289 eV[21,22] (Table 2). Aromatic aldehydes may also exhibit strong absorption near 288 eV,[19] again associated with the C=O $1s-\pi^*$ transition.

It is important to note that inclusion of the $1s-2\pi^*$ transitions from aromatic carbon is crucial when attempting to relate the apparent intensity of the absorption band at 289 to the concentration of aliphatic or other nonaromatic carbon. A sizable contribution to the total intensity around 289 eV is derived from these higher energy aromatic transitions.

Table 3. C-NEXAFS of Liptinite: Inner-Shell Transition Energies and Assignments

energy (eV)	assignment	carbon functionality
285	$1s-\pi^*$	$C_{AR}-H$, $C_{AR}-C$ (LUMO)
288	$1s-3p/\sigma_{C-H}^*$	CH_2, CH_3
289	$1s-\pi^*$	COOH, COOR
290	1s−4p	CH_2, CH_3
292	$1s-\sigma^*$	C−C (aliphatic)
294	$1s-\sigma^*$	C−C (aliphatic)
297	$1s-\sigma^*$	C−O (acid)

In addition to the higher energy aromatic $1s-\pi^*$ transitions (Figure 5) (Table 2), a low-intensity band positioned near 290.4 eV corresponding to the 4p Rydberg transition of alkyl carbon is also included (Table 2). The presence of such an absorption feature is inferred from the occurrence of absorption associated with the mixed valence/Rydberg (3p) transition near 288 eV.

At the highest energies, the asymmetric broad absorption band is deconvoluted into an aromatic carbon−carbon $1s-\sigma^*$ transition,[23] near 293 eV and a C−O $1s-\sigma^*$ transition near 297 eV [17] (Table 2). The asymmetric shapes of the bands on and above the ionization threshold are expected, the asymmetry resulting directly from lifetime broadening of the weakly bound excited state.[16] In Figure 5 symmetric Gaussian bands were added for simplicity, with the acknowledgment that asymmetric band shapes would be more correct. Table 2 presents an accounting of the energies and assignments of the observed and anticipated absorption edge fine structure for huminite.

The continuum step corrected spectrum for the liptinite macerals within this coal is presented in Figure 6 and is deconvoluted into seven component absorption bands. At the lowest energy a low-intensity absorption band centered near 285.6 eV is assigned to a $1s-\pi^*$ transition associated with sp^2-hybridized carbon (Table 3). Dominating liptinite's carbon spectrum, however, is an intense absorption band centered near 289 eV, which is a composite of at least three absorption bands. The first of these, centered near 288 eV, is assigned to a 1s transition to a Rydberg/C−H* state (Table 3). A strong absorption band in this energy region is commonly observed in normal and cyclic alkanes.[3,18]

The center absorption band, with E near 289 eV is assigned, principally, to a $1s-\pi^*$ transition of C=O groups (Table 3) associated with aliphatic acids and/or esters.[21,22] Aliphatic carboxylic acids and esters are essential constituents in the liptinite precursor materials and are expected to be present in liptinitic macerals within lower rank coals.

There may be a slight contribution to the intensity at 289 eV from a 1s−Rydberg/C−H* transition associated with aliphatic carbon α to the carbonyl of the acid or ester.[21,22] Assuming that the oscillator strength of mixed valence/Rydberg transitions is comparable for both types of aliphatic carbons and assuming that aliphatic carbon exceeds the concentration of C=O, then it is reasonable to conclude that contributions from this latter transition are minimal.

The high-energy side shoulder of the composite absorption band (Figure 6) results from an absorption band centered near 289.7 eV resulting from a 1s transition to the 4p Rydberg state of the methyl and

(23) Hitchcock, A. P.; Fischer, P.; Gedanken, A.; Robin, M. B. *J. Phys. Chem.* **1987**, *91*, 531.

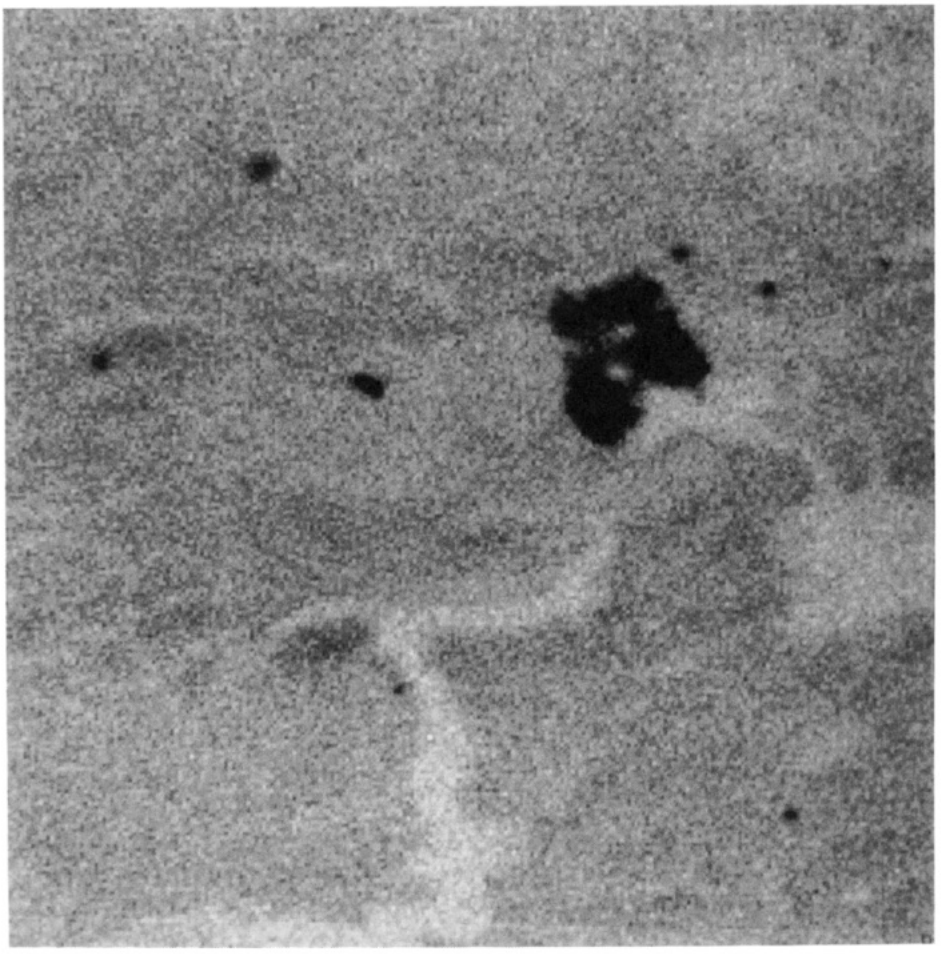

Figure 7. X-ray image of a selected region containing both liptinite and huminite. The monochromator is tuned to 270 eV corresponding to chlorine's 2s absorption edge. This energy is far below the lowest energy features associated with the carbon K edge.

methylene carbon (Table 3). Inner-shell spectra of highly aliphatic condensed phase materials such as poly(propylene) typically exhibit a pronounce shoulder near 290 eV[24] attributed to this transition. Similar spectral features have been observed in the inner-shell spectra of cyclohexane[3,25] and normal hexane,[18] supporting the assignment in the present case.

The broad region of absorption at the highest energies in Figure 6 results from the overlap of at least three absorption bands. The first is centered near 291 eV, the second near 294 eV, and the third near 297 eV. These absorption bands are assigned to 1s$-\sigma^*$ transitions, corresponding to aliphatic C$-$C and carboxylic C$-$O[3,18,21,22] (Table 3). Again, it should be noted that absorption bands above the ionization threshold are, usually, highly asymmetric. In the present case, however, Gaussian line shapes have been chosen to fit this region of the spectrum. If asymmetric line shapes were used, the mean energy, intensity, and line width would be expected to change somewhat.

Inorganic Precipitates in Huminite. Earlier discussions regarding Figure 1 drew attention to the highly absorbing region adjacent to the liptinitic maceral, observed when the monochromator was tuned to 285.5 eV. Lack of contrast observed between this region and the surrounding huminite at 288.1 eV in Figure 2 suggests that these regions are highly aromatic, perhaps inertinitic. However, another possibility exists; the intense absorption may result from an element other than carbon whose absorption edge lies in close proximity to carbons 1s absorption edge.

The chlorine 2s absorption edge is a potential candidate. Acquiring an image at an energy of 270 eV (Figure 7) confirms the presence of chlorine. Virtually all of the features observed previously in Figures 1 and 2 are now faint in Figure 7, except for the region which contains chlorine.

Scanning the energy range 260$-$280 eV yields the chlorine 2s NEXAFS spectrum composed of the absorption edge and a narrow intense band due to a transition to a 3p orbital (Figure 8). These data corroborate that the highly absorbing regions found in Figures 1 and 7 are clearly due to a localized concentrations of chlorine.

These chlorine-rich regions have been observed in all of the thin sections analyzed in the present study, including both the calcium-loaded and acid-washed (only) samples. It does not appear likely that such inclusions are primary constituents in this coal. Rather, it is reasonable to assume that chlorides formed as precipitates during the HCl wash. These observations raise an important issue regarding acid washing, namely, whether complete removal of all chelated cations from coal is possible. While acid washing undoubtedly leads

(24) Ade, H.; Zhang, X.; Cameron, S.; Costello, C.; Kirz, J.; Williams, S. *Science* **1992**, *258*, 972.

(25) Robin, M. B. *Higher Excited States of Polyatomic Molecules*; Academic Press, New York, 1974; Vol. I.

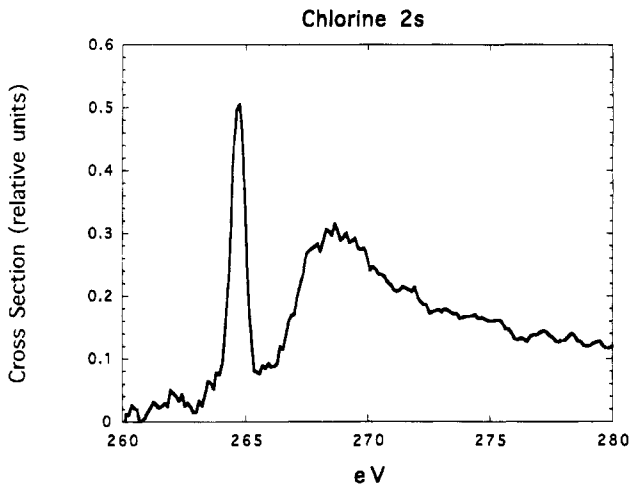

Figure 8. Cl(2s)-NEXAFS spectrum of the inorganic inclusion prominent in the X-ray images with the monochromator tuned to E = 285.5 and 270 eV, respectively.

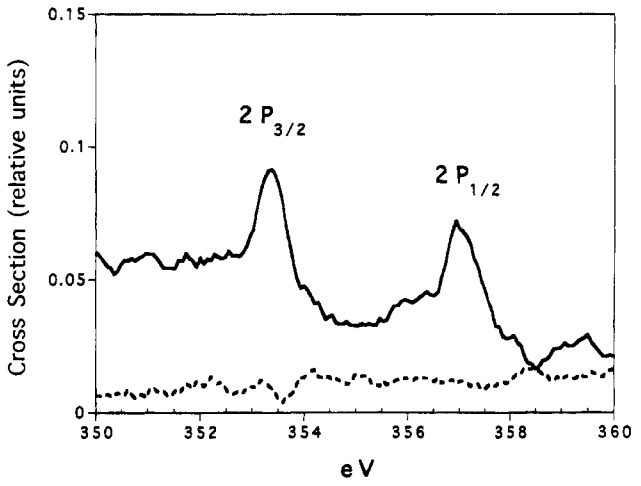

Figure 9. Ca(2p) spectra of the Ca^{2+}-loaded (solid line) and acid-washed huminite (dashed line). The two peaks in the Ca^{2+}-loaded specimen result from a single transition, energetically split by spin-orbital interactions.

to protonation of organic acids, the presence of chlorides indicates that transport of some solvated cations out of the coal may be severely diffusion limited.

Ca^{2+} Loading and Detection via Inner-Shell Spectroscopy. As stated previously, the energy range of calcium's 2p absorption edge is readily accessible at X1A. An inner-shell spectrum of Ca^{2+}-loaded huminite was obtained by scanning the energy range from 340 to 380 eV, this is presented in Figure 9. This same energy range was also scanned for a region of huminite from the acid-washed (only) sample. In the Ca^{2+}-loaded sample, two peaks are observed, separated by approximately 4 eV (Figure 9). These absorption bands correspond to transitions from calcium's 2p inner shell to a 3d excited state. The two peaks constitute spin-orbital partners, the splitting results from the interaction between the spin of the excited electron and the spin of ground state, 2p, orbital.[26] The energy difference between the $2p_{1/2}$ and the $2p_{3/2}$ transitions is on the order of what has been observed previously for calcium using XPS.[27] In the case of the acid-washed (only) huminite, no calcium was detected, indicating that the HCl rinse is capable of removing any exchangeable calcium in huminite.

Unfortunately, imaging on the calcium edge was not very interesting. The Ca^{2+}-loaded specimens were highly homogeneous and only the maceral huminite was observed. Calcium 2p absorption images obtained from within the huminitic matrix revealed no regions disproportionately rich in calcium. Clearly, the concentration of calcium in the liptinites would be expected to be different than that in huminite; however, the paucity of this maceral type in APCS No. 2 precluded our attempts to demonstrate this.

Although the calcium imaging failed to identify the presence of heterogeneities in the distribution of calcium within huminite, it served another useful, albeit unanticipated, function. Imaging on the calcium edge revealed that the chlorine-rich inclusions do not contain detectible quantities of calcium. Numerous inclusions observed throughout the samples when the monochromator was tuned near to the carbon K edge were not observed when images were acquired at the calcium edge. If the chloride inclusions do not contain Ca^{2+}, then the question arises regarding the identity of the cation. A probable candidate is chelated ferrous or even ferric iron which precipitated as chlorides following the HCl wash. It will be possible to validate this hypothesis using the STXM in the future because the Fe 2p absorption edge lies within the accessible energy window.

Conclusions

The results presented in this paper constitute a preliminary analysis of C-NEXAFS to obtain information on functional groups within compositionally discrete microdomains, macerals, in coal. In the case of huminite, aromatic, aliphatic, carboxylic, and hydroxylated aromatic carbon are clearly identified as principal constituents. Aliphatic and carboxylic carbon are identified as the principal constituents in liptinite. The enormous differences in the respective C-NEXAFS spectra of these two maceral types attest to the dissimilarity in their molecular structures.

In the future, spectral assignments will be refined as the sample set is expanded to include coals from lignite up to anthracite in rank. These data when combined with data derived from model compounds will enable a quantitatitive assessment of highly localized values for f_a, the average degree of ring hydroxylation, and carboxylic acid content, as a function of rank. A particularly promising area is the use of X-ray microspectroscopy to probe changes in the carbon spectra of coal macerals resulting from various reactions and processing conditions. In the near future, analysis will be extended to oxygen's K edge. Data acquired in this spectral range will unequivocally identify the oxygen functionality within compositionally discrete microdomains and facilitate the assignment of spectral features across the carbon near edge region to specific oxygen containing functional groups. Imaging on the oxygen edge has the potential to spectacularly reveal chemical heterogeneity within the lowest rank coals.

(26) Eyring, H.; Walter, J.; Kimball, G. E. *Quantum Chemistry*, John Wiley & Sons, Inc.: New York, 1967.

(27) Wagner, C. D.; Riggs, W. M.; Davis, L. E.; Moulder, J. E.; Muilenberg, G. E. *Handbook of X-ray Photoelectron Spectroscopy*, Perkin-Elmer, USA, 1979.

Acknowledgment. This work was performed at the National Synchrotron Light Source (NSLS) which is supported by the Department of Energy. G.D.C. gratefully acknowledges the Chemistry Division of Argonne National Laboratory for support granted through the award of the Enrico Fermi Scholarship. R.E.B. acknowledges support from the Office of Basic Energy Sciences, Department of Energy, under contract No. W-31-109-ENG-38. S.W. and the STXM Facility are supported by the Department of Energy, DOE/OHER, under contract No. 89ER60858. The authors extend their gratitude to Janos Kirz, Chris Jacobsen, and Xiadong Zhang of the Department of Physics, SUNY Stony Brook, for their assistance and to Russel Cook and Nestor Zaluzec of the Material Science Division, Argonne National Laboratory, for their assistance. The authors gratefully acknowledge A. P. Hitchcock and colleagues for their enormous contribution in the area of the carbon inner-shell spectroscopy of organic molecules. The analysis of the C-NEXAFS spectra of coal macerals could not proceed without reference to the data published over the past decade by these researchers.

EF9401987